Publication IV

Laura Koponen, Lasse O. Tunturivuori, Martti J. Puska, and Y. Hancock. 2010. Tunability of the optical absorption in small silver cluster–polymer hybrid systems. arXiv:1003.2183v3 [cond-mat.mtrl-sci]. The Journal of Chemical Physics, accepted for publication.

© 2010 by authors and © 2010 American Institute of Physics (AIP)

Preprinted by permission of American Institute of Physics.

arXiv:1003.2183v3 [cond-mat.mtrl-sci] 16 Apr 2010

Tunability of the optical absorption in small silver cluster–polymer hybrid systems

Laura Koponen[1],[1] Lasse O. Tunturivuori[1],[1] Martti J. Puska[1],[1] and Y. Hancock[1,21,a)]
[1] *Department of Applied Physics, Aalto University School of Science and Technology, P.O. Box 11100, FIN-00076 AALTO, Finland*
[2] *Department of Physics, The University of York Heslington, York, YO10 5DD, U.K.*

(Dated: 19 April 2010)

We have calculated the absorption characteristics of different hybrid systems consisting of Ag, Ag_2 or Ag_3 atomic clusters and poly(methacrylic acid) (PMAA) using the time-dependent density-functional theory. The polymer is found to have an extensive structural-dependency on the spectral patterns of the hybrid systems relative to the bare clusters. The absorption spectrum can be 'tuned' to the visible range for hybrid systems with an odd number of electrons per silver cluster, whereas for hybrid systems comprising an even number of electrons, the leading absorption edge can be shifted up to ~ 4.5 eV. The results give theoretical support to the experimental observations on the absorption in the visible range in metal cluster–polymer hybrid structures.

PACS numbers: 31.15.ag, 31.15.ee, 36.40.Vz, 82.35.Np

I. INTRODUCTION

When metal samples are reduced from bulk to nanometer dimensions, their optical properties become governed by surface plasmons. When the size is further decreased to few-atom clusters, the properties are again altered as discrete energy levels determine the electronic and optical behavior of the cluster[1,2]. Applications in this size regime have become extremely important during recent years as advanced experimental production on this scale has become more controlled and theoretical methods are now more easily able to access it[3,4].

Silver clusters are especially interesting but challenging materials. Their high biocompatibility suggests great potential as functional components in biological nanomaterials [5,6] with possible applications in biosensing and optical data processing[7–10]. Silver clusters readily oxidize, which can be a problem for some applications, and methods of increasing their stability against oxidation are actively being sought[11]. From the theoretical perspective, the challenge of these systems lies in the filled d-electron levels of silver, which makes high requirements for modeling their electronic properties, and for determining their potential for application.

During the last two decades, both extensive experimental and computational studies have been done on small silver clusters (Ag_n) with less than a dozen atoms. Experimentally these clusters have been studied in stabilizing rare-gas matrices, as free silver clusters in the gas phase dissociate by fragmentation[12–15]. Small silver clusters exhibit interesting luminescence and especially fluorescence properties that can be tuned by their size and chemical environment[16–18]. Interesting, but not very well understood, experimental observations on the tunability of their optical properties as a function of the chemical environment have been reported. Díez *et al.*, for example, have observed absorption in the visible range at ∼500 nm (2.5 eV) from small silver clusters ($n = 1 - 4$) stabilized by coils of poly(methacrylic acid) (PMAA) in the liquid phase[19]. The photoabsorption spectrum of this system was found to redshift slightly when the polarity of the solvent decreased, and other interesting properties, such as strong fluorescence and electrochemiluminescence, were also observed. A similar synthesis was also carried out by Shang *et al.*[20] who assumed that the measured absorption bands at 430 nm (2.9 eV) and 500 nm (2.5 eV) are due to Ag_n^+ clusters with $n = 2 - 8$. Their study also reported strong fluorescence.

On the computational side, methods used to model excited-state properties of nanosized structures include the coupled cluster method[21], *ab initio* configuration interaction (CI) approach[22], time-dependent density-functional theory (TDDFT)[23], Hedin's GW approach combined with the solution of the Bethe-Salpeter equation[24], and the quantum Monte Carlo method[25]. The quantum chemistry community, in particular, Bonačić-Koutecký *et al.* pioneered work on the absorption properties of silver clusters using *ab initio* CI, publishing many bench-mark results[22,26,27]. On the DFT side, Yabana and Bertsch were the first to use a real-time implementation of TDDFT to calculate the optical response of small silver clusters Ag_1, Ag_2, Ag_3, Ag_8 and Ag_9^+ in the gas phase[28]. A more systematic real-time TDDFT study of the optical properties of Ag_n with $n = 1 - 8$ followed[29]. Both of these studies showed good agreement with experimental results with a rather rigid difference of about 10% in the excitation energies. More recent TDDFT studies have been performed on larger Ag_n clusters with $n \geq 4$ [30–32].

A hybrid structure consisting of a silver cluster and an organic compound is of great interest as this is already a reliable model for a silver cluster that has been function-

a) Electronic mail: yh546@york.ac.uk

alized by its environment. Examples of studies on silver-cluster–organic-compound hybrid systems include silver-carboxylates for which DFT methods have been used to determine the shapes of the resulting silver nanoparticles[33,34]. The interaction with the organic compound can cause strong modifications to the optical properties of the cluster. For example, Mitrić *et al.* studied the absorption spectra of silver cluster–tryptophan hybrid systems using the TDDFT[35]. They observed a strong size- and structural-dependence of the photoabsorption and photofragmentation in these systems. Other examples of recent TDDFT work on silver-cluster–organic-compound hybrid structures include a study of the enhancement mechanism in surface enhanced Raman scattering[36–38] and the determination of the optical properties of silver-cluster–biomolecule-hybrids[39].

In this paper, we study the effect of organic compounds on the photoabsorption spectra of silver cluster systems. For our model systems, we choose clusters consisting of one to three silver atoms attached to fragments of the PMAA polymer. This choice is motivated by recent experiments in Refs.[19,20,40] where small silver clusters have been formed in the presence of PMAA in different solutions. In our calculations we focus on the cluster-polymer system only and omit the solvent for simplicity. This approach has also been used by Mitrić *et al.* who calculated the excitation properties of interacting nanoparticle-biomolecule subunits[35].

The paper is organised as follows. The selected geometries for our systems are investigated and presented in Sec. II. The DFT and TDDFT methods are covered in Sec. III. Sec. IV contains the results and the analysis of the ground-state calculations and Sec. V contains the results of the optical absorption (excited-state) calculations. Finally, the conclusions are given in Sec. VI.

II. STRUCTURES

In order to emphasize their essential features, a schematic representation of the structures we have studied is shown in Fig. 1. Full geometry optimization on these systems have also been performed, and the details of these calculations can be found in Sec. III. The acronyms used for these structures consist of a descriptive letter (P = polymer, M = monomer Ag_1 (atom), D = dimer Ag_2, T = trimer Ag_3) followed by a consecutive number. Our choice of systems for the hybrid structures is motivated by experimental evidence, which shows that carboxylate groups are capable of bonding with Ag ions in polyacids (see, e.g., Ref.[40] and references therein). Hence, in this work, our primary interest has been to study small (i.e., single atom and dimer) hybrids. For the monomer (M1–M8) and dimer (D1–D7) structures, a large variety of different geometries have been systematically studied, whereas only a few trimer structures (T1–T2) have been used to test whether the trends obtained for monomer atom and dimer structures can be extended for systems containing larger Ag_n clusters.

The pure polymer (P1–P4) and pure cluster (M1, D1 and T1) geometries are used as reference systems throughout this work. A simple, representative structure for a polymer-cluster hybrid system has one Ag_n cluster attached to the polymer-monomer unit, for example, R–$COO^-Ag_n^+$ (M2, D2 and T2). We also consider more complicated structures where the Ag_n cluster is between the carboxylate groups of two such polymer-monomers (M7 and D6). Here, the Ag_n cluster is bound to four oxygen atoms, which create a stabilizing environment for it.

The case of longer polymer chains bonded to Ag_1 monomers and Ag_2 dimers is also addressed. Two questions arise regarding the spectral properties of these systems. First, does the length of the polymer chain itself have an effect on the absorption characteristics of the Ag_n cluster (M2 vs. M3 or M4, and D2 vs. D3 or D4)? Second, are the clusters attached to nearby branches of the system interacting with each other (M2–M4 vs. M5 and M6 or M7 vs. M8, and D6 vs. D7)?

When considering longer polymer chains, the concept of tacticity plays an important role in determining the lowest-energy structures. For a pure polymer, both iso- (P3) and syndiotactic (P4) isomers were considered. A similar comparison can be made between M3 and M4 as well as between D3 and D4, even though the chain lengths are not equal. All of the structures with three polymer units in a row were chosen to be syndiotactic for two reasons. First, there is experimental evidence to suggest that the systems are likely to be syndiotactic[19]. Second, isotactic polymer chains with Ag_n clusters attached to neighboring polymer units tend to aggregate to form larger clusters. Thus, isotactic polymer chains do not favor the formation of stable hybrid structures with the small Ag_n clusters that are studied here. In the case of Ag_2 clusters, the neighboring clusters aggregate even when they are attached to the next-neighbor polymer units for both iso- and syndiotactic polymers. The unstable structure D5 is shown in Fig. 1 as an example to high-light this point. In comparison, the structure D7 in which both dimers have stable anchorings to two polymer chains is found stable.

The relative energies of the different structures were not studied in detail as it is not possible to compare the energetics of systems having different numbers and types of atoms. A direct energy comparison can only be made between the structures M2 and D6, and between the structures M5 and D7. In these cases, the D6 and D7 structures are favoured in energy by at least 1 eV per Ag atom.

III. COMPUTATIONAL METHODS

The SIESTA program[41], which implements the standard Kohn-Sham self-consistent density-functional method, was used in spin-dependent calculations for the

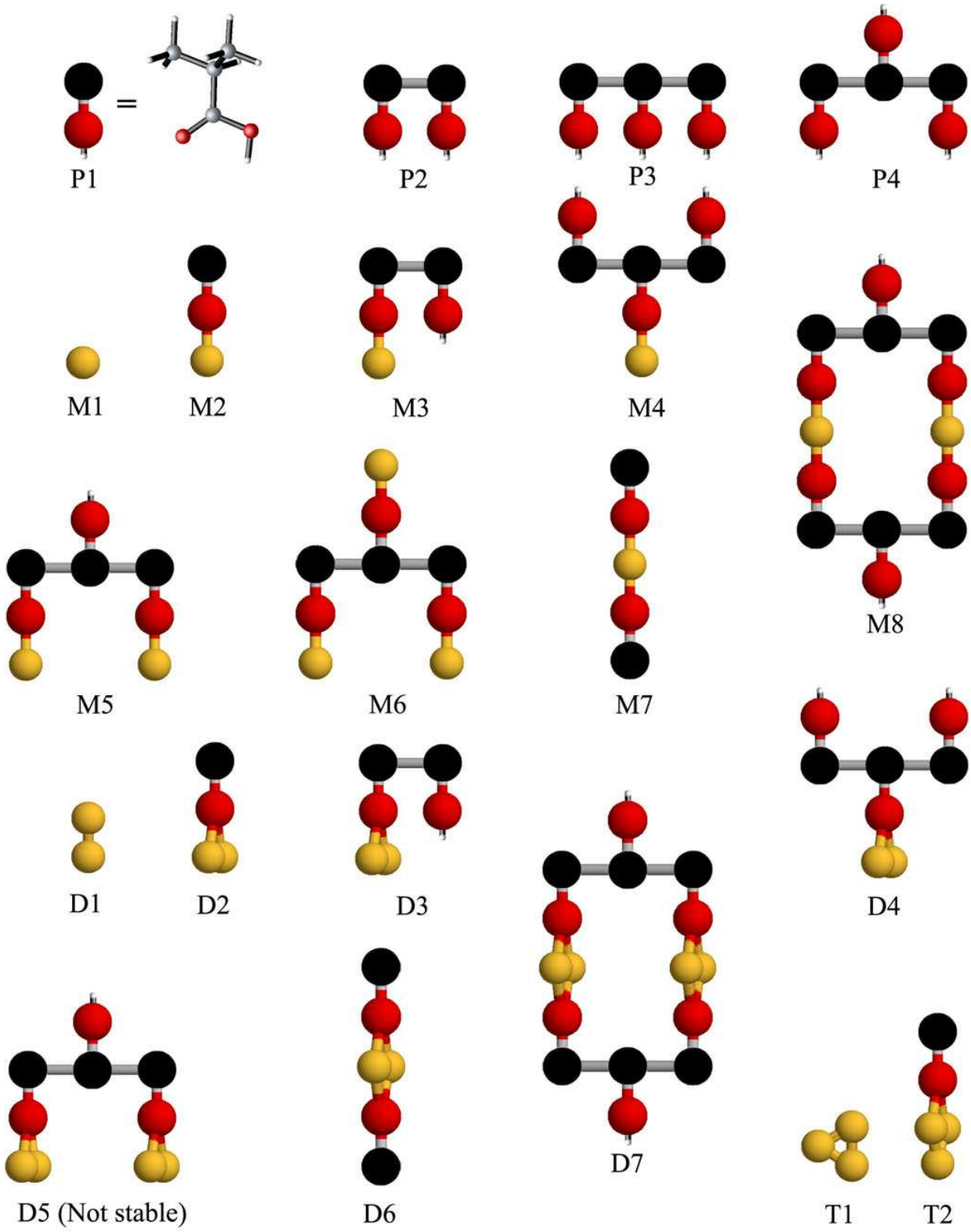

FIG. 1. (Color) Schematic pictures of studied structures (not to scale). Black, dark red, tiny white and small yellow dots represent PMAA units, their carboxylate groups, the hydrogen atoms of the carboxyl groups, and Ag atoms, respectively. The bond lengths or bond angles in the pictures do not represent the calculated values except for the detailed illustration of polymer-monomer P1, where large grey, large dark red and small light grey dots represent the carbon, oxygen and hydrogen atoms, respectively.

geometry optimizations. The Perdew-Burke-Ernzerhof (PBE) generalized gradient approximation (GGA)[42], Troullier-Martins pseudopotentials[43], and the double zeta plus polarization (DZP) basis-set were also used in this work. The SIESTA program optimizes the geometries of the systems through a series of atomic displacements, until the calculated forces on the atoms are less than 0.01 eV/Å. This is the standard procedure for geometry optimization using the SIESTA code, in which the numerical "noise", e.g., due to the real-space grid in the potential calculation, prevents the geometry optimization from being stuck at high-symmetry saddle points. Hence, in this work, Hessian analysis was not used for the structural optimization.

The TDDFT program OCTOPUS[44] (version 3.0.0/3.0.1) was applied in all further ground-state and excited-state calculations. Real-time TDDFT (RT-TDDFT) in its various flavors has been successfully used to determine the spectral properties of a large variety of both metal clusters and organic compounds[45]. Calculating optical absorption spectra by TDDFT and comparing them with the measured spectra has proven to be an efficient tool for determining cluster and molecule structures, and even distinguishing between different isomers (see, e.g., Refs.[46,47]). In most cases, a good agreement with experiments up to a few tenths of an eV in spectral features is achieved.

In this work, we used the RT-TDDFT method as implemented in OCTOPUS to calculate the absorption spectra in the linear response regime. The RT-TDDFT implementation follows Ref.[48], where the system is instantaneously excited by applying an electric field, and the occupied Kohn-Sham orbitals are then propagated in time. The photoabsorption cross-section follows from the induced dipole moments, and is calculated separately for each of the three spatial directions. The RT-TDDFT method should not be confused with linear-response TDDFT (LR-TDDFT) methods, such as the Casida method[49]. LR-TDDFT methods are superior for calculations of small systems. However, due to their poor scaling, the RT-TDDFT method becomes advantageous for large systems as it scales linearly with respect to the electron number. In this study, the Casida LR-TDDFT method within OCTOPUS was used to resolve the specific transitions contributing to the absorption spectra for systems M1, M2, D1, and D2.

The PBE exchange-correlation functional was used in the TDDFT calculations, except in the Casida calculations, where the available kernel in OCTOPUS corresponds to the local density approximation (LDA). Troullier-Martins pseudopotentials[43] were used in all of the TDDFT calculations in this work. The calculations in the OCTOPUS program are based on a real-space grid. We used a spacing of 0.23 Å for the real-space grid, and a simulation radius around each atom of 8 Å, which are typical values in real-space RT-TDDFT calculations. The validity of the grid-spacing was verified by reference calculations for the test structure M2 using grid-spacings of 0.17 Å and 0.20 Å. All three grid-spacings produced similar absorption spectra up to an accuracy of about 0.1 eV in the relevant low-energy region of about 0–7 eV. All relevant characteristics of the spectra were clearly resolved using this accuracy, as the low-energy excitations of small metal clusters are well-spaced. The obtained numerical accuracy is also within the general accuracy of a few tenths of an eV for this method[23,46]. The time-step for the calculation was 0.0025 $\hbar$/eV and the number of time-steps was 20000 for the pure Ag_n clusters and the PMAA-monomer structure and 15000 for the rest of the structures, resulting in a total propagation time of 50 $\hbar$/eV $\approx$ 33 fs / 37.5 $\hbar$/eV $\approx$ 25 fs. In the Casida calculations, the number of unoccupied states that were taken into account was 4.2 times the number of occupied states for the largest structure D2 and at least 8 times the number of occupied states for the other structures. These numbers were considered adequate to produce reliable results for the D2 structure and high-quality results for all of the other systems.

TABLE I. Properties of the studied systems. Even (odd) denotes even (odd) number of electrons per Ag_n cluster. All bond lengths are given in Ångströms. Cluster-cluster distances are in italics.

Structure	Even/Odd	Ag-O	Ag-Ag
M1	Odd	–	–
M2	Even	2.32–2.34	–
M3	Even	2.32–2.42	–
M4	Even	2.33–2.34	–
M5	Even	2.33–2.34	–
M6	Even	2.32–2.35	–
M7	Odd	2.25–2.27	–
M8	Odd	2.25–2.28	*6.62*
D1	Even	–	2.581
D2	Odd	2.27–2.32	2.709
D3	Odd	2.26–2.28	2.710
D4	Odd	2.27–2.28	2.709
D6	Even	2.17	2.781
D7	Even	2.17	2.786, *6.52*
T1	Odd	–	2x2.644, 3.023
T2	Even	2.24–2.25	2x2.74, 2.723

IV. GROUND-STATE RESULTS

The calculated bond lengths for the Ag containing structures are shown in Table I. In the case when the dimer is attached to the polymer, the Ag-Ag bonds are slightly lengthened (D1 vs. D2–D7). For the trimer, the Ag-Ag bond lengths in the triangle become almost equal (T1 vs. T2). The Ag-O bond lengths vary only slightly between 2.17–2.42 Å in the different structures, which is somewhat longer than the 2.04 Å bond length in bulk silver oxide Ag_2O[50].

The ground-state calculations also give the HOMO-LUMO energy gaps, which can be considered as zeroth-

order approximations to the first excitation energy. We found that the structures of the same type, i.e., those having the same cluster size and the same number of polymer chains (for example, M2–M6 and D2–D4), have energy gaps of similar size. On the other hand, a strong gap variation exists between structures of different types. An odd number of electrons per Ag_n cluster is found to introduce a HOMO-LUMO energy gap smaller than 1.5 eV in all of the polymer-containing structures, whereas all polymer-containing structures with an even number of electrons per Ag_n cluster have gaps that are larger than 1.85 eV. Even though M8 has a total number of electrons that is even, the odd number of electrons per Ag_1 monomer in this system leads to local magnetic moments in the vicinity of the two Ag atoms, and to a HOMO-LUMO energy gap that is smaller than 1.0 eV. For comparison, Refs.[51,52] also report on calculated HOMO-LUMO energy gaps smaller than 1 eV for odd-electron Ag_n clusters within the size range of $n = 2 - 20$. The exception to this trend is the single silver atom (M1 in our notation), which has a gap that is greater than 3 eV.

V. EXCITED-STATE RESULTS

The absorption spectra for the pure polymer structures are given in Fig. 2. Each system shows a similar spectrum with an absorption edge above 4.5 eV. In the energy range of 4.5–7 eV, several peaks appear with slightly varying patterns depending on the type of structure. The spectra of structures P3 and P4, which differ only by tacticity, are almost identical in this energy range. The largest spectral strengths for these systems appear at higher energies ranging up to several tens of eV's. This region, which is above the ionization energies of these systems, is not included in this figure as it is beyond the range of application of the TDDFT method.

The absorption spectra corresponding to structures with monomers Ag_1, dimers Ag_2 and trimers Ag_3 are shown in Figs. 3, 4 and 5, respectively. The pure Ag_n clusters, M1, D1 and T1, have their main lowest excitation energies at 3.8 eV, 3.0/4.5 eV and 2.5/2.8/3.3/3.6 eV, respectively, in excellent agreement with previous studies[28,29].

The inclusion of the PMAA monomer in structures M2 and T2 causes only slight changes of a few tenths of an eV in the position of the lowest excitation and a slight decrease in its intensity relative to those of the Ag monomer M1 and trimer T1, respectively (cf. M1 and M2 in Fig. 3 and T1 and T2 in Fig. 5). In addition, the spectral features of the polymer above 4.5 eV appear in both the M2 and T2 cases. In contrast, for the dimer D2 in Fig. 4, the main low-energy excitations are perturbed with new excitations appearing at surprisingly low energies of 1.7 eV and 2.1 eV. From the individual directional components of the spectrum (not shown in the figure), it can be concluded that these two low-energy excitations are caused

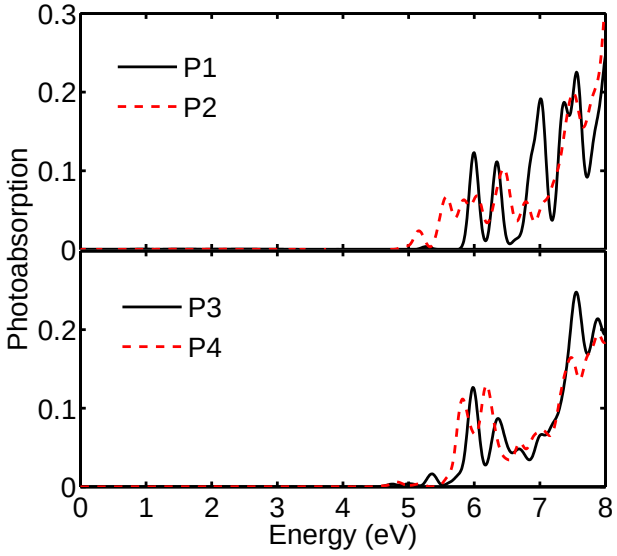

FIG. 2. (Color) Photoabsorption spectra of the pure polymer structures. The absorption strengths are scaled down by a factor of 1/2 for P2 and 1/3 for P3 and P4 to compensate for the different system sizes.

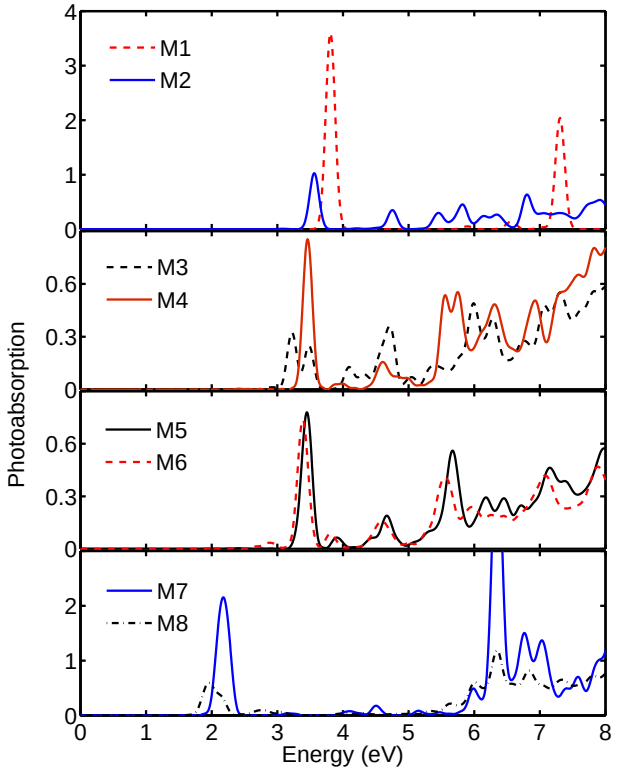

FIG. 3. (Color) Photoabsorption spectra of the structures with Ag_1 monomers. The absorption strengths are scaled down by a factor of 1/2 or 1/3 for systems containing 2 or 3 Ag atoms, respectively, to compensate for the different system sizes. Note the different y-axis scales.

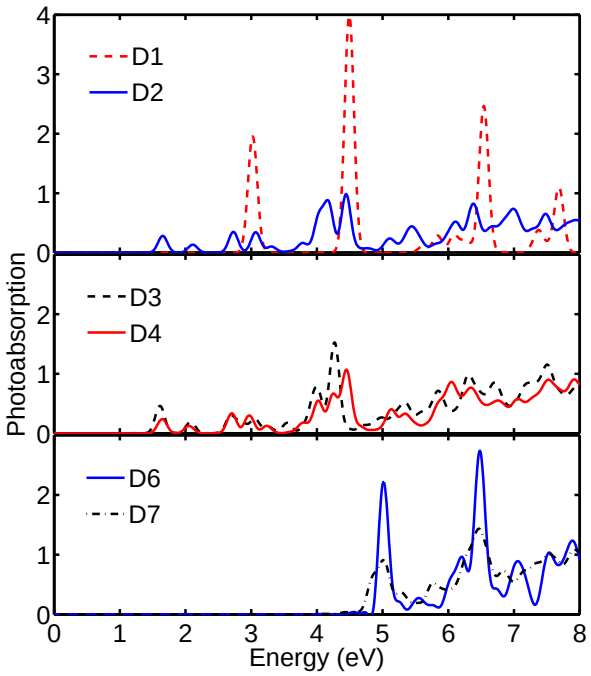

FIG. 4. (Color) Photoabsorption spectra of the structures with Ag_2 dimers. The absorption strength is scaled down by a factor of 1/2 for D7 to compensate for the different system size.

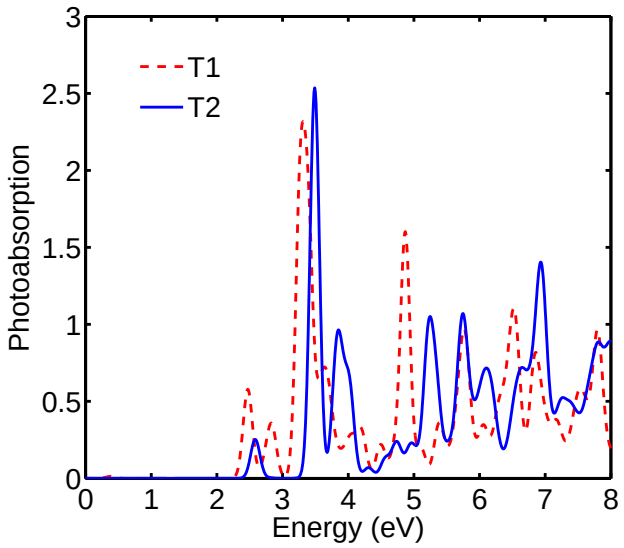

FIG. 5. (Color) Photoabsorption spectra of the structures with Ag_3 trimers.

by charge oscillations in the dimer-axis direction, whereas the excitations at 2.7–4.5 eV are along all three spatial directions. To compare, the pure dimer D1 excitation at 3.0 eV stems from the dimer-axis direction, and the doubly-intense excitation at 4.5 eV arises from the two other degenerate spatial directions perpendicular to the dimer-axis. Hence, we conclude that both low-energy peaks in the pure dimer spectrum have been destroyed and are replaced by a new pattern of multiple low-energy peaks in the spectrum of the D2 structure. We conjecture that this change in the low-energy spectrum arises due to the odd number of electrons in the vicinity of the Ag_n cluster corresponding to the perturbation in the electronic structure induced by the polymer. Such a perturbation is already reflected in the ground-state results, for example, in the widths of the HOMO-LUMO energy gaps.

Elongating the polymer chain causes only minor changes in the spectra. For example, compared to the single polymer-monomer systems M2 and D2, the spectra for the corresponding asymmetric structures M3 and D3 containing chains of two polymer-monomers, and the structures M4 and D4 containing chains of three polymer-monomers, differ only slightly (see Figs. 3 and 4). Neighboring Ag_n clusters do not significantly affect the spectrum either. This can be seen, for example, in Fig. 3 by comparing the spectrum of the M5 structure consisting of the syndiotactic chain of three polymer-monomers and the Ag atoms attached to next-neighbor polymer-monomers, with that of the structure M6 with the syndiotactic chain of three polymer-monomers and the Ag atoms attached to each of the polymer-monomers. Only a slight redshift of about 0.1 eV and an extra shoulder at about 2.7–2.9 eV are observed in the latter case. To summarize, adding polymer units or even Ag atoms in M3–M6 does not change the fundamental trends in the spectra compared to M2. The same holds for the dimer structures D2–D4.

When the Ag_n clusters are surrounded by two PMAA chains, dramatic changes in the absorption spectra are observed. For example, the low-energy excitations of M7 and M8 correspond to the odd number of electrons per Ag_n cluster in the hybrid structure. This is similar to the odd electron number effect seen in the D2, D3 and D4 systems, which resulted in low-energy excitations. For the Ag monomer structure M7 (Fig. 3), the main low-energy excitation appears at 2.2 eV. Thus, this excitation is about 1.3 eV lower in energy than the low-energy excitations in M2–M6. The structure M8, which contains two such clusters at a mutual distance of 6.6 Å, shows a moderate splitting and a slight redshift of the main excitation with respect to M7.

In the case of dimers that are surrounded by two polymer chains (D6 and D7, Fig. 4), an opposite effect is observed. Namely, the absorption edge is brought up to over 4 eV. The low-energy excitation of the pure Ag dimer D1 (Fig. 4) at about 3 eV in the dimer-axis direction is totally suppressed in the spectra for the D6 and D7 systems. The main excitations at about 5 eV and 6.5 eV for the D6 and D7 systems arise from the direction of the "bridges" between the two polymer chains. Thus, the presence of the polymer causes quenching of

the low-energy absorption of the Ag_2 dimer. Because no quenching was observed when Ag_n clusters were attached to single polymer chains (M2–M6, T2), we deduce that the formation of the symmetric structure of the Ag_n cluster and the four oxygen atoms in the D6 and D7 systems plays a key role in the suppression of certain directional vibration modes.

To examine the origin of the shifts in the excitation spectra, the photoabsorption spectra of the smallest structures M1, M2, D1 and D2 were calculated using the Casida method. This enables us to determine which orbitals are involved in the excitations, as such information is not directly available from the RT-TDDFT calculations. The compositions of the main low-energy excitations of M2, D1 and D2 are shown in Figs. 6a–8a. For the pure Ag monomer M1, the transition from the HOMO to the triply degenerate LUMO makes a 95% contribution to the low-energy excitation. Note that an almost constant shift of about 0.3 eV in transition energies between Figs. 3–4 and 6a–8a is caused by the use of the LDA kernel instead of the PBE kernel in the Casida calculations. To demonstrate the extent of the electronic perturbation induced by the polymer, the orbital illustrations of a few orbitals around the gap are also shown in Figs. 6b–8b, where the orbitals are illustrated as constant-value surfaces of the electron wavefunctions.

Fig. 6a shows that the main low-energy excitation in the absorption spectrum of M2 corresponds to the transitions from the HOMO-1 and HOMO-2 orbitals to the LUMO orbital. As shown in Fig. 6b, these orbitals are localized over the carboxylate group and the Ag atom, and even over the carbon skeleton. This differs clearly from the pure Ag atom HOMO-LUMO excitation from the s-orbital to the triply degenerate p-orbital.

For the Ag dimer D1, the LUMO is an anti-bonding orbital and the degenerate LUMO+1 and LUMO+2 are π-bonding orbitals as can be seen in Fig 7. A similar pattern with a clear interaction between the Ag dimer and the carboxylate group is seen in the orbitals of the D2 structure in Fig. 8. The difference between D1 and D2 is that D2 has an odd number of electrons, and a net spin resulting in an absorption spectrum with several excitations at lower energies. Previous results by Mitrić *et al.*[35] for Ag_n cluster–tryptophan structures show similar features to our findings. For the Ag dimer attached to the carboxylate group of a tryptophan molecule, an excitation at an anomalously low energy of about 2.3 eV was observed[35]. This effect was associated with a HOMO-LUMO transition that is similar to the one described above for our system, D2.

Next, we consider the quenching of the lowest excitation peak when moving from the dimer D1 to structures D6 and D7 (See Fig. 4). The increase in the bond length between the Ag atoms is far too small to explain the quenching. Instead, we note that the HOMO-LUMO transition makes a 94% contribution (Fig. 7) to this excitation. The quenching that is observed is therefore due to the destruction of the σ shape of the HOMO, which happens already in the D2 structure as seen in Fig. 8.

Finally, we want to consider the charge transfer as a possible source of error in our calculations. The effect of charge transfer can lead to errors of several eV's in excitation energies for the commonly used (semi)local functionals such as PBE[53]. The hybrid functionals such as B3LYP do not perform much better. To probe the reliability of the PBE functional in our calculations, we have used the criterion by Peach *et al.* to estimate the amount of charge transfer[53]. In this criterion, Peach *et al.* define the spatial overlap Λ as attaining values between 0 and 1, so that large values correspond to low charge transfer. According to Peach *et al.* the PBE results are predicted to be reliable for $\Lambda > 0.4$. We found that for the structure M2, Λ is for the lowest energy excitation within the range of 0.50–0.54. For the structure D2, the Λ values for the five low-energy excitations shown in Fig. 8a are, in the order of increasing excitation energy, within the ranges of 0.71–0.73, 0.60–0.63, 0.60–0.62, 0.43–0.46 and 0.61–0.64, respectively. The uncertainty in these values is due to the inclusion of a limited number of orbitals in the calculation of Λ. From these values and the orbital illustrations in Figs. 6 and 8, we conclude that the character of the transitions is mainly local, and that the PBE functional can be safely used to study the main features of the excitations in these systems. To see whether the same conclusion can be drawn for our larger systems, we have examined the electronic structure of M5. We observe that the orbitals near the gap of this system have shapes similar to those of M2 (See Fig. 6). Moreover, each of the orbitals of M5 is totally or mainly localized in the vicinity of one Ag atom only. Supported by the previous result that the photoabsorption spectra changed only slightly with the chain length, we can conclude that the excitations of M5 are also local in character. Using the structure D2 as a reference, a similar analysis was also performed for D6, which yielded the same result. As the rest of the structures have a strong resemblance to these test cases, we do not expect the charge transfer to be a major source of error in any of the excitations in the studied structures.

VI. CONCLUSIONS

We have studied how the photoabsorption spectra of Ag_1, Ag_2 and Ag_3 clusters are affected by the presence of the PMAA polymer. The structure optimization shows that there exists stable configurations in which the Ag_n clusters are bound to the carboxylate group of the polymer.

We observe that the bonding of the polymer to the Ag_n clusters has an extensive effect on the absorption characteristics in certain cases. Namely, when the number of electrons per Ag_n cluster is odd, the electronic structure and thereby the spectral features of the Ag_n clusters are strongly perturbed. For example, for the $PMAA^-Ag_2^+$ systems with an odd number of electrons, the minimum

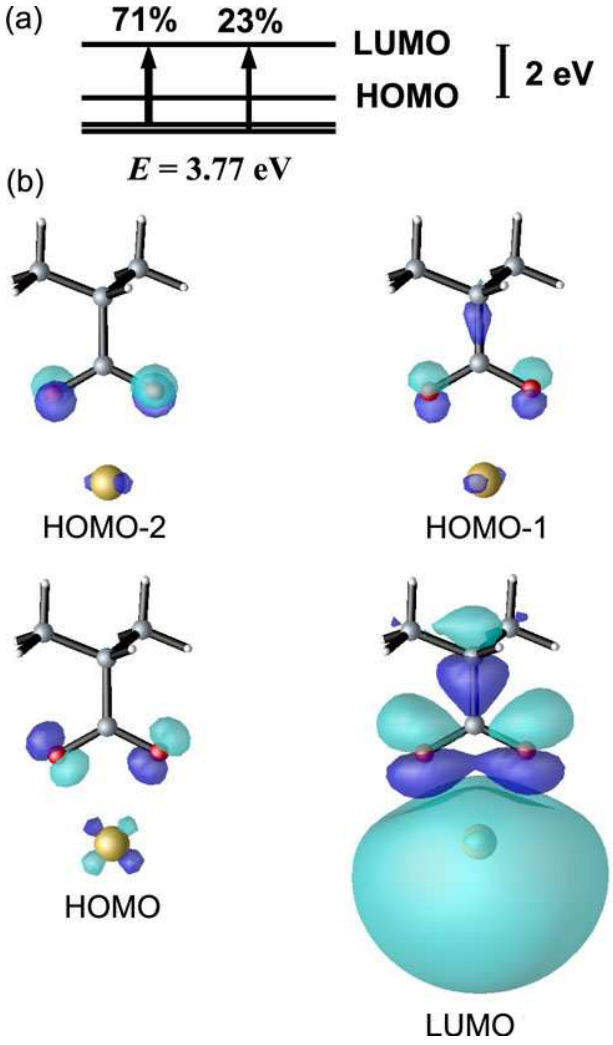

FIG. 6. (Color) (a) Energy level diagram of the main low-energy excitation at energy E and (b) orbital illustrations of the structure M2. Light blue represents positive and dark blue negative parts of the wavefunction.

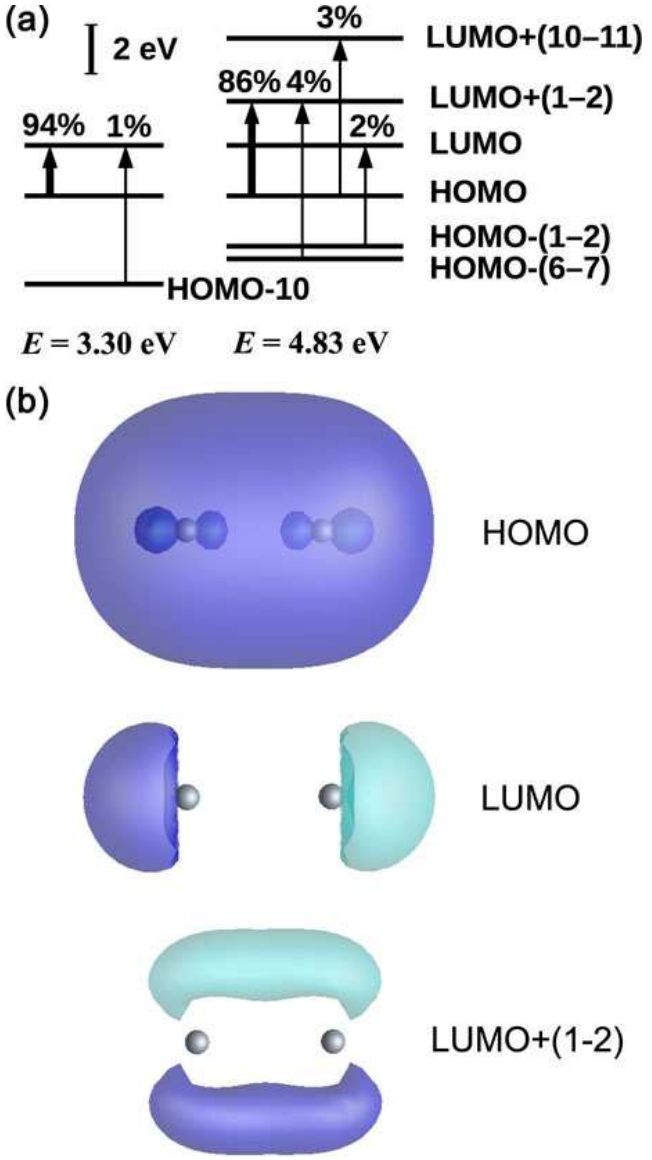

FIG. 7. (Color) (a) Energy level diagram of the main low-energy excitations at energies E and (b) orbital illustrations of Ag dimer D1. The excitation at $E = 4.83$ eV is doubly degenerate as the LUMO+1 and LUMO+2 states are degenerate orbitals. Light blue represents positive and dark blue negative parts of the wavefunction. Reference energy level diagrams can be found in Refs.[29,30].

absorption energy is lowered by almost 1.5 eV resulting in absorption in the visible range. Suppression of the lowest excitations is observed when an Ag_n cluster with an even number of electrons, such as Ag_2, is surrounded by two carboxyl groups, so that the cluster is bonded to four oxygen atoms.

Our results reveal that the absorption features of the smallest Ag_n clusters are very sensitive to their chemical environment. This suggests that these clusters are viable candidates for materials with tailored optical properties. Already, there exists experimental evidence on the ability to tune the absorption and emission spectra of small Ag_n cluster–polymer hybrid systems. The results presented here give theoretical confirmation of those findings, thus showing such systems to be promising candidates for developing functional nanomaterials with adjustable properties.

ACKNOWLEDGMENTS

This research is supported by the Academy of Finland through the Centers of Excellence Program (2006–2011). CSC, the Finnish IT center for science, is acknowledged for providing computer resources (project tkk2035). We thank Robin Ras and Isabel Díez for introducing us the experimental motivation of this study and Risto Nieminen for discussions.

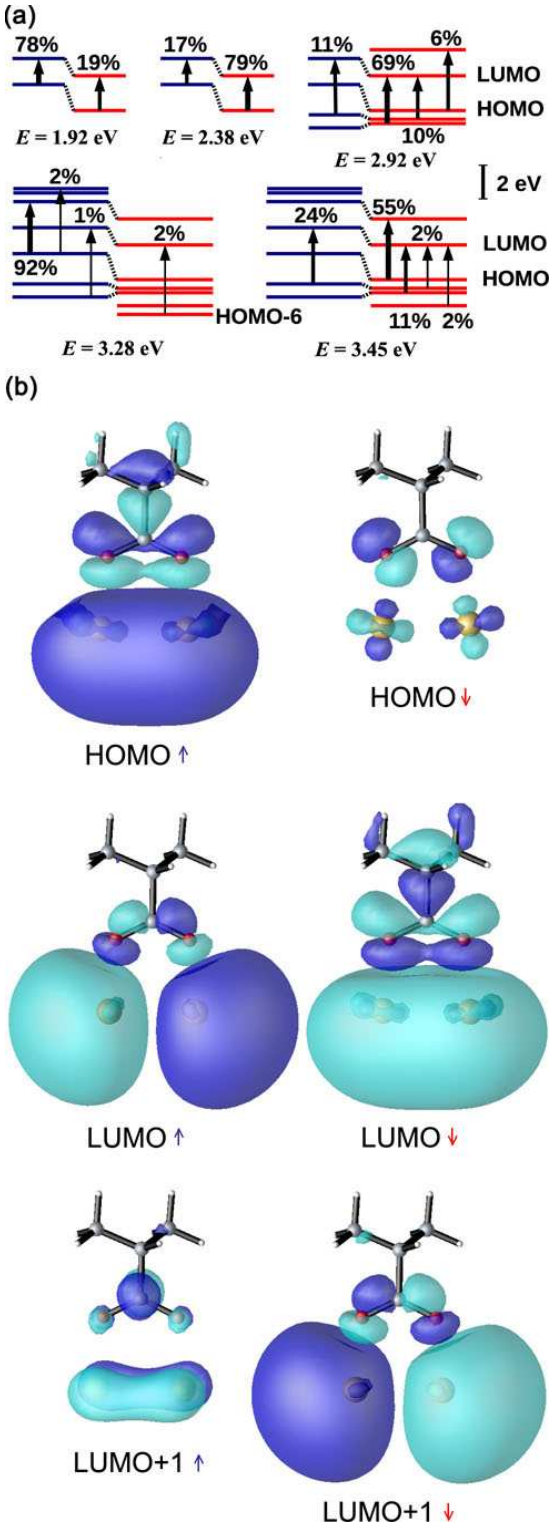

FIG. 8. (Color) (a) Energy level diagram of the main low-energy excitations at energies E and (b) orbital illustrations of the structure D2. The left and right (blue and red) energy levels represent the two different spin populations. Light blue marks the positive and dark blue the negative parts of the wavefunction.

[1] G. Schmid, Advanced Engineering Materials **3**, 737 (2001).
[2] J. Zheng, P. R. Nicovich, and R. M. Dickson, Annu. Rev. Phys. Chem. **58**, 409 (2007).
[3] W. Greiner, and A. Solov'yov, Chaos, Solitons and Fractals **25**, 835 (2005).
[4] F. Balletto, and R. Ferrando, Rev. Mod. Phys. **77**, 371 (2005).
[5] J. T. Petty, J. Zheng, N. V. Hud, and R. M. Dickson, J. Am. Chem. Soc. **126**, 5207 (2004).
[6] J. M. Slocik, J. T. Moore, and D. W. Wright, Nano Lett. **2**, 169 (2002).
[7] L. Peyser-Capadona, J. Zheng, J. I. González, T.-H. Lee, S. A. Patel, and R. M. Dickson, Phys. Rev. Lett. **94**, 058301 (2005).
[8] T. Gleitsmann, B. Stegemann, and T. M. Bernhardt, Appl. Phys. Lett. **84**, 4050 (2004).
[9] L. A. Peyser, T.-H. Lee, and R. M. Dickson, J. Phys. Chem. B **106**, 7725 (2002).
[10] T.-H. Lee and R. M. Dickson, Proc. Natl. Acad. Sci. U.S.A. **100**, 3043 (2003).
[11] W. Cai H. Zhong and L. Zhang, J. Appl. Phys. **83**, 1705 (1998).
[12] W. Harbich, S. Fedrigo, F. Meyer, D. M. Lindsay, J. Lignieres, J. C. Rivoal, and D. Kreisle, J. Chem. Phys. **93**, 8535 (1990).
[13] S. Fedrigo, W. Harbich, and J. Buttet, Phys. Rev. B **47**, 10706 (1993).
[14] W. Schulze, I. Rabin, and G. Ertl, ChemPhysChem **5**, 403 (2004).
[15] F. Conus, V. Rodrigues, S. Lecoutre, A. Rydlo, and C. Félix, J. Chem. Phys. **125**, 024511 (2006).
[16] L. A. Peyser, A. E. Vinson, A. P. Bartko, and R. M. Dickson, Science **291**, 103 (2001).
[17] C. Félix, C. Sieber, W. Harbich, J. Buttet, I. Rabin, W. Schulze, and G. Ertl, Phys. Rev. Lett. **86**, 2992 (2001).
[18] J. Zheng and R. M. Dickson, J. Am. Chem. Soc. **124**, 13982 (2002).
[19] I. Díez, M. Pusa, S. Kulmala, H. Jiang, A. Walther, A. S. Goldmann, A. H. E. Müller, O. Ikkala, and R. H. A. Ras, Angew. Chem. Int. Ed. **48**, 2122 (2009).
[20] L. Shang and S. Dong, Chem. Comm. **2008**, 1088 (2008).
[21] J. Čižek, J. Chem. Phys. **45**, 4256 (1966).
[22] V. Bonačić-Koutecký, L. Češpiva, P. Fantucci and J. Koutecký, J. Chem. Phys. **98**, 7981 (1993).
[23] M. A. L. Marques, C. A. Ullrich, F. Nogueira, A. Rubio, K. Burke, and E. K. U. Gross, eds., *Time-Dependent Density Functional Theory* (Springer-Verlag, Berlin Heidelberg, 2006).
[24] G. Onida, L. Reining, and A. Rubio, Rev. Mod. Phys. **74**, 601 (2002).
[25] W. M. C. Foulkes, L. Mitas, R. J. Needs, and G. Rajagopal, Rev. Mod. Phys. **73**, 33 (2001).
[26] V. Bonačić-Koutecký, J. Pittner, M. Boiron, and P. Fantucci, J. Chem. Phys. **110**, 3876 (1999).
[27] V. Bonačić-Koutecký, V. Veyret, and R. Mitrić, J. Chem. Phys. **115**, 10450 (2001).
[28] K. Yabana and G. F. Bertsch, Phys. Rev. A **60**, 3809 (1999).
[29] J. C. Idrobo, S. Öğüt, and J. Jellinek, Phys. Rev. B **72**, 085445 (2005).
[30] M. L. Tiago, J. C. Idrobo, S. Öğüt, J. Jellinek, and J. R. Chelikowsky, Phys. Rev. B **79**, 155419 (2009).
[31] G. F. Zhao, Y. Lei, and Z. Zeng, Chemical Physics **327**, 261 (2006).
[32] M. Harb, F. Rabilloud, D. Simon, A. Rydio, S. Lecoultre, F. Conus, V. Rodrigues, and C. Félix, J. Chem. Phys. **129**, 194108 (2008).
[33] L. P. Olson, D. R. Whitcomb, M. Rajeswaran, T. N. Blanton,and B. J. Stwertka, Chem. Mater. **18**, 1667 (2006).
[34] D. S. Kilin, O. V. Prezhdo, and Y. Xia, Chem. Phys. Lett. **458**, 113 (2008).
[35] R. Mitrić, J. Petersen, A. Kulesza, and V. Bonačić-Koutecký, J. Chem. Phys. **127**, 134301 (2007).
[36] S. M. Morton, and L. Jensen, J. Am. Chem. Soc. **131**, 4090 (2009).
[37] J. Zhao, L. Jensen, J. Sung, S. Zou, G. C. Schatz, and R. P. Van Duyne, J. Am. Chem. Soc. **129**, 7647 (2007).

[38] L. Jensen, L. L. Zhao, and G. C. Schatz, J. Phys. Chem. C **111**, 4756 (2007).
[39] T. Tabarin, A. Kulesza, R. Antoine, R. Mitríc, M. Broyer, P. Dugourd, and V. Bonačić-Koutecký, Phys. Rev. Lett. **101**, 213001 (2008).
[40] R. Konradi and J. Rühe, Macromolecules **38**, 4345 (2005).
[41] J. M. Soler, E. Artacho, J. D. Gale, A. García, J. Junquera, P. Ordejón, and D. Sánchez-Portal, J. Phys.: Condens. Matter **14**, 2745 (2002), http://www.uam.es/departamentos/ciencias/fismateriac/siesta/.
[42] J. P. Perdew, K. Burke, and M. Ernzerhof, Phys. Rev. Lett. **77**, 3865 (1996).
[43] N. Troullier and J. L. Martins, Phys. Rev. B **43**, 1993 (1991).
[44] A. Castro, H. Appel, M. Oliveira, C. A. Rozzi, X. Andrade, F. Lorenzen, M. A. L. Marques, E. K. U. Gross, and A. Rubio, Phys Status Solidi B **243**, 2465 (2006), http://www.tddft.org/programs/octopus/.
[45] P. Elliott, K. Burke, and F. Furche, Rev. Comput. Chem. **26**, 91 (2008).
[46] A. Castro, M. A. L. Marques, J. A. Alonso, and A. Rubio, J. Comput. Theor. Nanosci. **1**, 230 (2004).
[47] A. Castro, M. A. L. Marques, J. A. Alonso, G. F. Bertsch, K. Yabana, and A. Rubio, J. Chem. Phys. **116**, 1930 (2002).
[48] K. Yabana and G. F. Bertsch, Phys. Rev. B **54**, 4484 (1996).
[49] M. E. Casida, in *Recent Developments and and Application of Modern Density Functional Theory*, edited by J. M. Seminario (Elsevier, Amsterdam, 1996), pp. 391–439.
[50] R. W. G. Wyckoff, *Crystal Structures*, vol. 1 (John Wiley & Sons, New York, London, 1963), 2nd ed.
[51] J. Zhao, Y. Luo, and G. Wang, Eur. Phys. J. D **14**, 309 (2001).
[52] M. Pereiro, D. Baldomir, and J. E. Arias, Phys. Rev. A **75**, 063204 (2007).
[53] M. J. G. Peach, P. Benfield, T. Helgaker, and D. J. Tozer, J. Chem. Phys. **128**, 044118 (2008).